Letter

Temperature-induced miscibility of impurities in trapped Bose gases

G. Pascual,[1] T. Wasak,[2] A. Negretti,[3] G. E. Astrakharchik,[1] and J. Boronat[1]

[1]*Departament de Física, Universitat Politècnica de Catalunya, Campus Nord B4-B5, E-08034 Barcelona, Spain*

[2]*Institute of Physics, Faculty of Physics, Astronomy and Informatics, Nicolaus Copernicus University in Toruń, Grudziądzka 5, PL-87-100 Toruń, Poland*

[3]*Zentrum für Optische Quantentechnologien, Fachbereich Physik, Luruper Chaussee 149, D-22761 Hamburg, Germany*

(Received 22 December 2023; accepted 14 March 2024; published 16 April 2024)

We study the thermal properties of impurities embedded in a repulsive Bose gas under a harmonic trapping potential. In order to obtain the exact structural properties in this inhomogeneous many-body system, we resort to the path-integral Monte Carlo method. We find that, at low temperatures, a single impurity is expelled to the edges of the bath cloud if the impurity-boson coupling constant is larger than the boson-boson one. However, when the temperature is increased, but still in the Bose-condensed phase, the impurity occupies the center of the trap and, thus, the system becomes miscible. This thermal-induced miscibility crossover is also observed for a finite concentration of impurities in this inhomogeneous system. We find that the transition temperature for miscibility depends on the impurity-boson interaction and we indicate a different nondestructive method to measure the temperature of a system based on the studied phenomenon.

DOI: 10.1103/PhysRevResearch.6.L022014

Introduction. The Bose polaron has been extensively studied both at zero temperature [1–22] as well as at finite temperatures [23–28]. Such a system presents a significant interest not only due to fundamental questions about quasiparticle formation, but also the mobility of the impurity inside the Bose-Einstein condensate (BEC), as was recently shown, can serve as a *nondestructive* indicator of the temperature of the whole system [29]. However, the question of how a single impurity behaves in an inhomogeneous BEC at finite temperature was not addressed.

In homogeneous repulsive Bose-Bose mixtures, the mean-field approximation provides a robust criterion to distinguish miscible and immiscible phases at zero temperature. In particular, if $g_{\rm BB}$, $g_{\rm II}$, and $g_{\rm BI}$ denote the intra- and interspecies coupling constants, respectively, the two components of the mixture are phase separated when $g_{\rm BI} > \sqrt{g_{\rm BB} g_{\rm II}}$ and they are mixed when $g_{\rm BI} < \sqrt{g_{\rm BB} g_{\rm II}}$ [30]. Quantum Monte Carlo (QMC) techniques have verified this criterion and, moreover, they have extended the analysis to finite temperatures revealing that Popov theory fails in describing repulsive Bose mixtures at finite polarization [31–34]. Nevertheless, an inhomogeneous thermal mixture has only been studied, using QMC techniques, in Ref. [35] with the same number of particles per species.

The behavior of an impurity in an inhomogeneous gas at finite temperature and the effect of the number of impurities in the miscibility of the system are topics that have yet to be addressed in the field. QMC techniques can shed some light on it and provide novel methods for thermometry.

In the present Letter, our main goal is to study the thermal properties of impurities immersed into an inhomogeneous Bose gas. We use the path-integral Monte Carlo method (PIMC) which provides an exact technique to find structural properties such as the density profile in an exact way, within controllable statistical errors. We analyze the system for different interaction strengths between the impurity and the rest of the particles, and we observe that above a certain interaction $g_{\rm BI}$ the impurity remains outside the Bose gas (see Fig. 1). Finally, we observe the existence of a mixing temperature above which the impurity penetrates the center of the gas.

Model. The Hamiltonian of the $(N + N_{\rm I})$-particle system in a harmonic trap in three dimensions is given by

$$H = -\frac{\hbar^2}{2m}\sum_{i=1}^{N}\nabla_i^2 - \frac{\hbar^2}{2m}\sum_{I=1}^{N_{\rm I}}\nabla_{\rm I}^2 + \sum_{i<j}^{N} V_{\rm BB}(r_{ij}) + \sum_{i,I}^{N,N_{\rm I}} V_{\rm BI}(r_{iI}) + \sum_{I<J}^{N_{\rm I}} V_{\rm II}(r_{IJ}) + \sum_{n=1}^{N} V_{\rm ext}(r_i) + \sum_{I=1}^{N_I} V_{\rm ext}(r_I), \tag{1}$$

where lowercase (uppercase) indices denote particles (impurities) with positions r_α and distances $r_{\alpha\beta} = |r_\alpha - r_\beta|$ between them, with $\{\alpha, \beta\} = \{i, I\}$. We consider an experimentally relevant case where all the particles have the same mass m. We model the repulsive boson-boson (impurity-impurity) interaction potential by $V_{\rm BB}(r) = V_{\rm II}(r) = V_0/r^{12}$ and boson-impurity by $V_{\rm BI} = V_0^{\rm BI}/r^{12}$ with amplitudes V_0 and $V_0^{\rm BI}$ chosen to reproduce [36,37] the desired values of the s-wave scattering length a and $a_{\rm BI}$, correspondingly. The coupling constants, which appear in the mean-field theory, $g = g_{\rm BB} = g_{\rm II}$ and $g_{\rm BI}$,

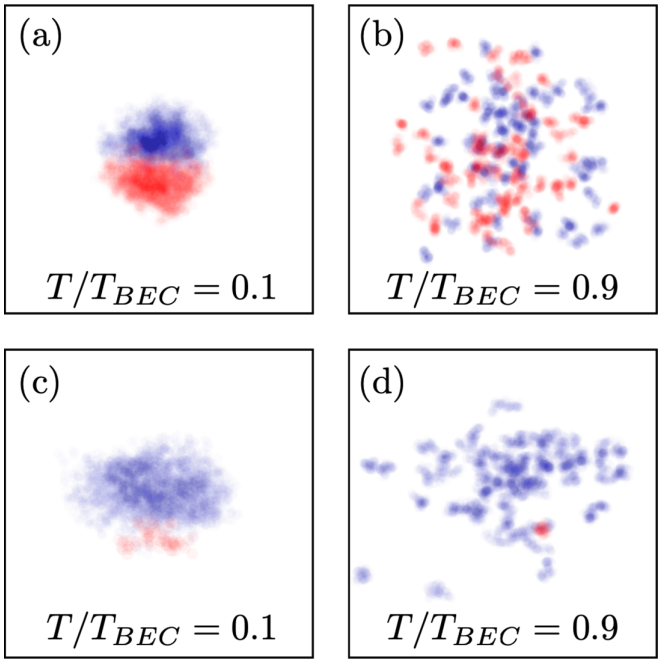

FIG. 1. Snapshots of PIMC positions of the beads of particles (blue) and impurities (red) for different characteristic parameters. (a) and (b) correspond to a binary mixture with the number of particles equal to the number of impurities, $N_{\rm I} = N$, $g_{\rm BI}/g = 3.5$, and $g_{\rm BB} = g_{\rm II} = g$. (c) and (d) show a single impurity with $g_{\rm BI}/g = 4.5$ in a bath. The systems are immiscible at $T/T_{\rm BEC} = 0.1$ and are miscible at $T/T_{\rm BEC} = 0.9$, being $T_{\rm BEC}$ defined in Eq. (2).

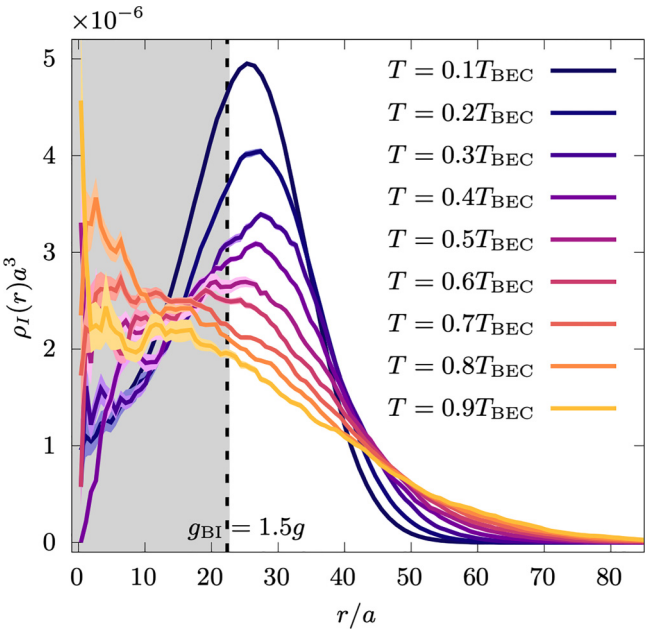

FIG. 2. Single-impurity density profile in a bath containing $N = 64$ bosons with $g_{\rm BI}/g = 1.5$ and $a_{\rm ho}/a = 15$ is depicted using various colors, each corresponding to a different temperature. The density profile is normalized to the number of impurities ($N_{\rm I} = 1$ in this case). The dashed vertical line shows the most probable impurity position as approximated by Eq. (5). The gray area shows where half of the particles of the bath are located at $T = 0.1T_{\rm BEC}$ (in Appendix A we show the density profiles). Notice that the impurity starts penetrating the center of the trap as the temperature is increased.

are related to a and $a_{\rm BI}$ within the first Born approximation as $g = 4\pi\hbar^2 a/m$, and similarly for $g_{\rm BI}$. The external confinement is taken in the form of a harmonic trap with frequency ω, i.e., $V_{\rm ext}(r) = m\omega^2 r^2/2$, which defines a characteristic oscillator length scale set by $a_{\rm ho} = \sqrt{\hbar/(m\omega)}$. For sufficiently low values of the gas parameter, na^3, the specific shape of the interaction potential is no longer important and the description in terms of the s-wave scattering length becomes universal [38]. To ensure that the simulations are performed in this universal regime, we ascertain that the density n_0 at the center of the trap in our simulations is sufficiently low, $n_0 a^3 < 10^{-5}$. This is achieved by setting $a_{\rm ho}/a = 15$ while using around 100 particles. The temperature scale is set by the degeneracy temperature of an ideal BEC in a harmonic trap, which depends solely on the number of particles N and the trap frequency ω, i.e.,

$$k_B T_{\rm BEC} = \hbar\omega \left(\frac{N}{\zeta(3)} \right)^{1/3}, \tag{2}$$

where $\zeta(x)$ is the Riemann zeta function.

Method. We perform PIMC simulations of N bosons and $N_{\rm I}$ impurities in a three-dimensional (3D) harmonic trap [see Eq. (1)]. In this method, the kinetic and the potential parts of the temperature density matrix are decoupled and a Trotterization algorithm is applied [39]. In this scheme, the exponential of the Hamiltonian is divided into small divisions (called *beads*) in such a way that the thermal density matrix can be approximated into decoupled terms by using fourth-order expansions such as the Chin action [40,41]. This technique has been used in other works exploring dilute mixtures at finite temperature in which structural properties of the system have been computed accurately [28,34]. The indistinguishability of the bosonic particles is imposed by sampling permutations using the worm algorithm [42]. In this algorithm, particles, represented as polymers, where each *subparticle* corresponds to a different bead (i.e., the particle at a particular imaginary time), can be cut, bound, and swapped to other polymers making the overall chain a cluster of indistinguishable particles. We note that we have verified that doubling the number of particles does not lead to any significant change in the observed phenomena.

Results. In order to study the effects of the temperature, we focus on experimentally observable structural properties, such as the density profile of the impurity. The density profiles shown in the following figures have been all computed using the PIMC method explained above. In Fig. 2, we report for a system with a single impurity ($N_{\rm I} = 1$) various density profiles obtained by changing the temperature while keeping the ratio of the coupling constants fixed to $g_{\rm BI}/g = 1.5$. Remarkably, at low temperatures, the impurity remains mostly outside of the central region of the trap in which the bath density is maximal. This effect emerges from a delicate balance between the repulsive interactions and potential energy of the external harmonic trapping, since by expelling the impurity, its energy associated with the external potential is increased, while the energy coming from the interaction with bath particles is decreased. The contribution of the impurity to the potential

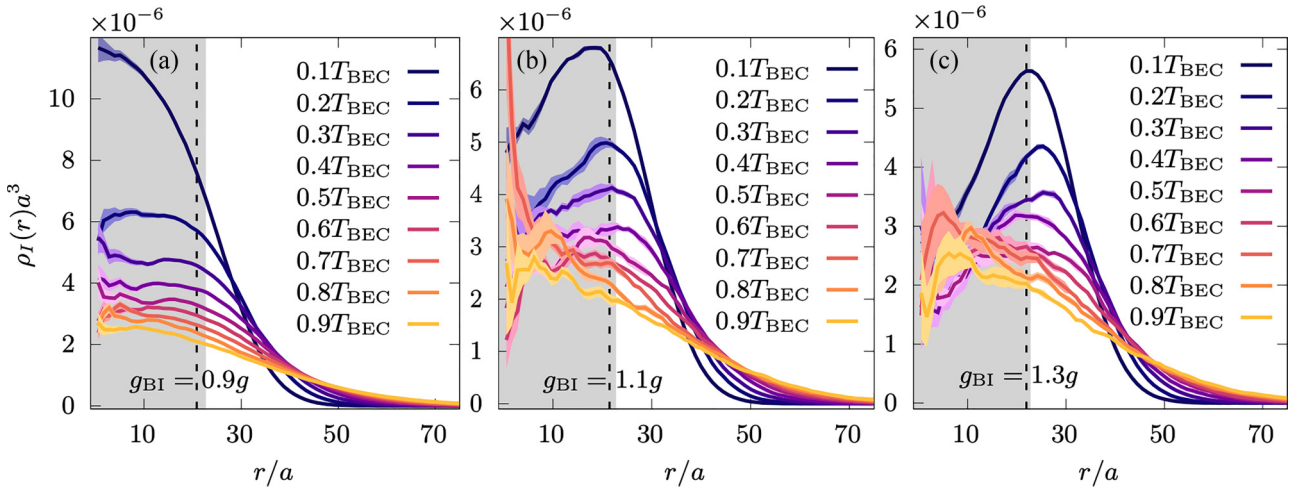

FIG. 3. Single-impurity density profile, similar to Fig. 2 but for various values of $g_{\rm BI}/g$, including values both larger and smaller than 1.

energy can be roughly estimated by assuming that the boson-impurity interaction is weak and the impurity profile $\rho_{\rm I}(\mathbf{r})$ does not modify the density profile of the bath $\rho_{\rm B}(\mathbf{r})$,

$$E_{\rm I} = \int d\mathbf{r} \int d\mathbf{r}_I \rho_{\rm B}(\mathbf{r})\rho_{\rm I}(\mathbf{r}_I)V_{\rm BI}(|\mathbf{r}-\mathbf{r}_I|) + \int d\mathbf{r}\rho_{\rm I}(\mathbf{r})V_{\rm ext}(\mathbf{r}), \tag{3}$$

where $\rho_{\rm B}(\mathbf{r})$ can be taken as the ideal Bose gas density at $T=0$, i.e., $\rho_{\rm B}^{\rm IG}(r) = N/(\pi^{3/2}a_{\rm ho}^3)\exp(-r^2/a_{\rm ho}^2)$. Equation (3) can be further simplified by assuming that the boson-impurity interaction is a contact pseudopotential, $V_{\rm BI}(\mathbf{r}) \to g_{\rm BI}\delta(\mathbf{r})$, and the impurity is located at a certain distance from the center, $\rho_{\rm I}(\mathbf{r}) \propto \delta(x-r_{\rm I})\delta(y)\delta(z)$, where we arbitrarily choose the direction of the impurity as the x axis. Within these approximations, one gets

$$E_{\rm I} = g_{\rm BI}\,\rho_{\rm B}^{\rm IG}(r_I) + V_{\rm ext}(r_I). \tag{4}$$

The most probable position of the impurity, $r_{\rm I}$, is then defined by minimization of its potential energy (4),

$$\frac{r_I}{a_{\rm ho}} = \sqrt{\ln\left(\frac{8}{\pi^{1/2}}\frac{Na_{\rm BI}}{a_{\rm ho}}\right)}. \tag{5}$$

This prediction for the most probable position of the impurity is shown in Fig. 2 with a vertical dashed line. A reasonably good agreement is found in the cases when the impurity is expelled from the center, which happens for low T. For strong boson-impurity interactions (i.e., $g_{\rm BI}/g \gg 1$), Eq. (5) loses accuracy because it is derived by assuming an absence of correlations and, moreover, the impurity starts to significantly modify the density profile of the bath.

Another limiting factor to our approximation is that in Eq. (5) we assumed a noninteracting bath. However, for a significantly larger number of particles, such that $(Na/a_{\rm ho})^{1/5} \gg 1$, the local density approximation (LDA) is expected to be applicable and the zero-temperature density profile of the bath would instead take a form of an inverted parabola [43].

As the temperature of the system is increased, we find that at a mixing temperature ($T = T_m$) the impurity fully penetrates the center of the trap. We define T_m as the temperature at which the peak in the density profile of the impurity moves from a finite value to the center of the trap. The mixing temperature T_m depends on the coupling constant $g_{\rm BI}$; for example, we find $T_m/T_{\rm BEC} = 0.6 \pm 0.1$ for $g_{\rm BI}/g = 1.5$, and $T_m/T_{\rm BEC} = 0.8 \pm 0.1$ for $g_{\rm BI}/g = 4.5$. We emphasize that in all our calculations T_m is lower than the degeneracy temperature $T_{\rm BEC}$, which means that this phenomenon appears in the condensed phase.

Since the mean-field criterion for a miscible to immiscible transition, expressed as $g_{\rm BI} = \sqrt{g_{\rm BB}g_{\rm II}}$, is not applicable to a single impurity due to the absence of a defined value of $g_{\rm II}$, we investigate miscibility as a function of the ratio $g_{\rm BI}$ and $g = g_{\rm BB}$. To this end, in Fig. 3 we plot the density profiles of the impurity for various T and $g_{\rm BI}/g$. We find that when $g_{\rm BI}/g < 1$ the impurity remains miscible with the rest of the particles at the center of the trap, while for $g_{\rm BI}/g > 1$ we observe the same immiscible behavior as in Fig. 2, i.e., at low T the impurity is repelled from the central region of the trap and it penetrates the center when the temperature increases. We note that the estimated position of the impurity with Eq. (5) works well in the immiscible phase while it fails in the miscible one.

To explore the influence of multiple impurities on temperature-induced miscibility, we study $N_{\rm I} > 1$ impurities interacting with each other with the same interatomic potential as the particles in the bath, i.e., $V_{\rm II}(r) = V_{\rm BB}(r)$. In Appendix B, we study the effect of N on the system. In Fig. 4, we show characteristic density profiles of the impurities for various number of impurities $N_{\rm I}$, focusing on the case of strong atom-impurity interactions ($g_{\rm BI}/g = 3.5$). At low temperatures the immiscible phase is formed. For small impurity concentration, the impurities are expelled outside creating a spherically symmetric shell and completely voiding the central region at $r = 0$ [see Fig. 4(a)], similarly to the single-impurity case. As the impurity concentration is increased, the outer shell broadens due to impurity-impurity interactions, as can be seen by comparing Figs. 4(a) and 4(b), while the spherical symmetry is still preserved. Instead, in the balanced case, $N_{\rm I} = N$, a phase with a different symmetry is realized [35,44], composed of two blobs of pure phase, each occupying one half of the trap. The interface surface between impurities and particles is minimized as it corresponds to a

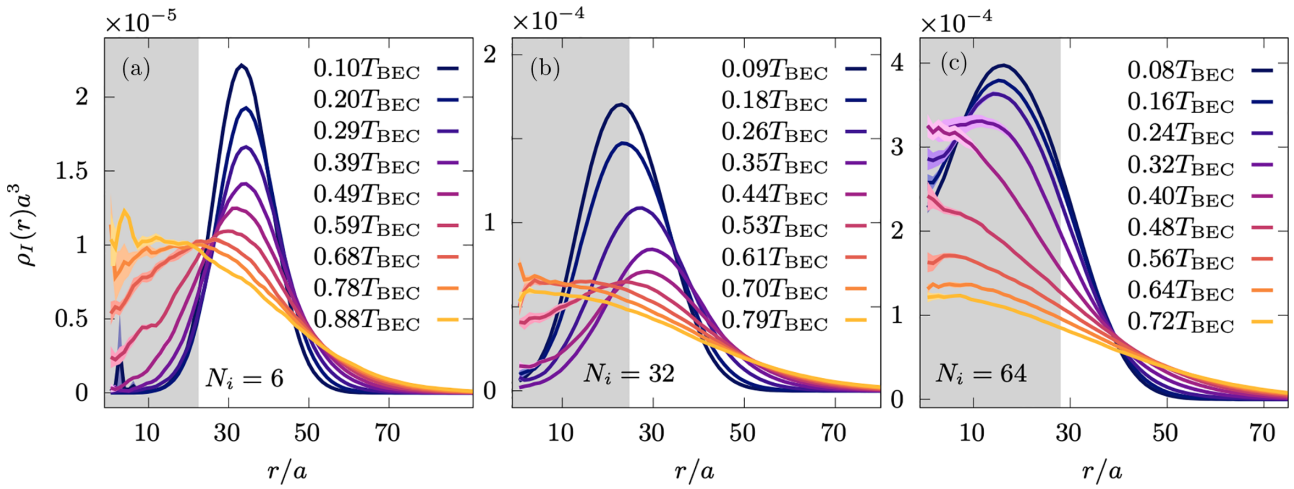

FIG. 4. Multiple-impurity density profile in a bath containing 64 bosons with $g_{\mathrm{BI}}/g = 3.5$ and $a_{\mathrm{ho}}/a = 15$. The density profiles are normalized to the number of impurities ($N_{\mathrm{I}} = 6; 32; 64$), in increasing order from left to right. The gray area shows where half of the particles of the bath are located at $T = 0.1T_{\mathrm{BEC}}$.

flat circle rather than to a sphere. A typical snapshot of the two-blob phase is shown in Fig. 1(a) and it has the $r = 0$ region fully accessible for the impurities as manifested by large values of $\rho_{\mathrm{I}}(r = 0)$ [Fig. 4(c)]. As the temperature is increased, the system changes its symmetry and undergoes a crossover to a miscible phase.

Finally, in Fig. 5 we study strongly repulsive interactions between the impurity and the rest of the particles. For large g_{BI}/g ratios, the strong boson-impurity repulsion causes the impurity to be expelled to a larger radius, as can be expected from Eq. (5). At the same time, more energy is needed to overcome the interaction with the bath (i.e., to occupy the center of the trap) and, as a consequence, the mixing temperature T_m grows. This result indicates that T_m has a significant dependence on g_{BI}.

Conclusions and discussion. In this Letter, we address the polaron problem by performing PIMC simulations of impurities immersed in a bosonic gas within a harmonic trap. We compute the density profile of the impurity at finite temperatures. We find that even though the mean-field criterion for homogeneous mixtures [30] is not defined in the single-impurity case, we observe miscible and immiscible regimes. At low temperatures, the impurity fully penetrates the central region of the bath cloud for $g_{\mathrm{BI}}/g < 1$, while the bosonic bath expels the impurity to the outer shell for $g_{\mathrm{BI}}/g > 1$. Notably, this result goes beyond the quasiparticle picture where the impurity is surrounded and dressed by excitations of the bath. The observed phenomenon recalls what happens in droplets of ^{4}He when impurities of ^{3}He are added to the system [45,46]. These impurities are also expelled to the surface of the droplet creating what is known as the Andreev state [47,48]. Furthermore, we have found a closed expression that approximates the most probable distance of the impurity from the center. This prediction holds well for the immiscible phase ($g_{\mathrm{BI}}/g > 1$) as long as the repulsion is not very strong. Instead, for strong impurity-atom interactions and large impurity concentration the system loses spherical symmetry and splits into two blobs.

As the temperature of the system is increased, we observe a critical temperature T_m above which the mixing occurs and the impurity fully penetrates the center of the trap. We discover a noticeable dependence of T_m on the coupling constant g_{BI}. The more repulsive the impurity, the higher is the mixing temperature T_m. This phenomenon can be used in experiments to estimate the temperature of the system without disturbing it. Notice that, as it has been shown in our work, the insertion of the impurity to the system barely modifies the properties of the bath and, thus, this method is *nondestructive*. The relation

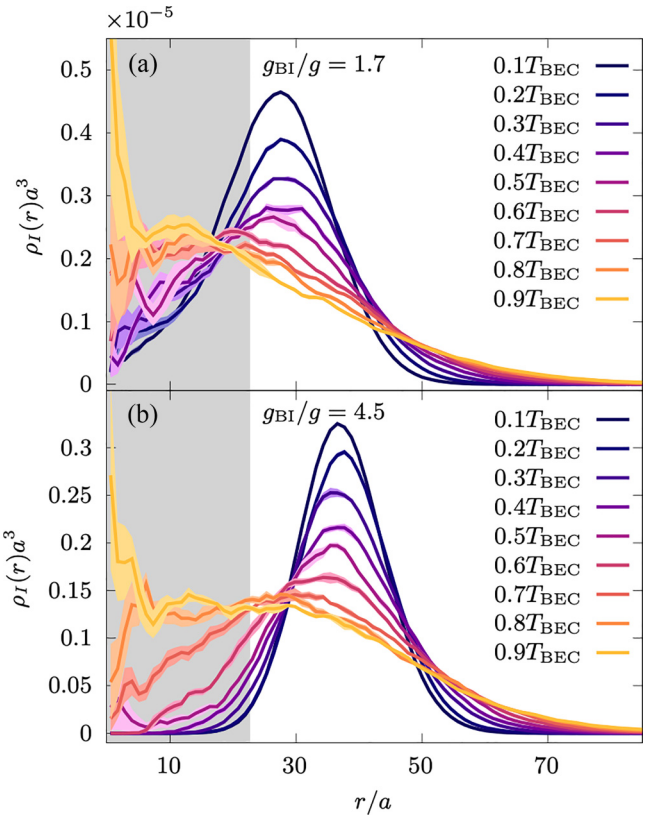

FIG. 5. Density profiles of the impurity interacting repulsively with a bath of 64 bosons at different g_{BI}/g and with $a_{\mathrm{ho}}/a = 15$. The density profile is normalized to the number of impurities ($N_{\mathrm{I}} = 1$ in this case). The gray area shows where half of the particles of the bath are located at $T = 0.1T_{\mathrm{BEC}}$.

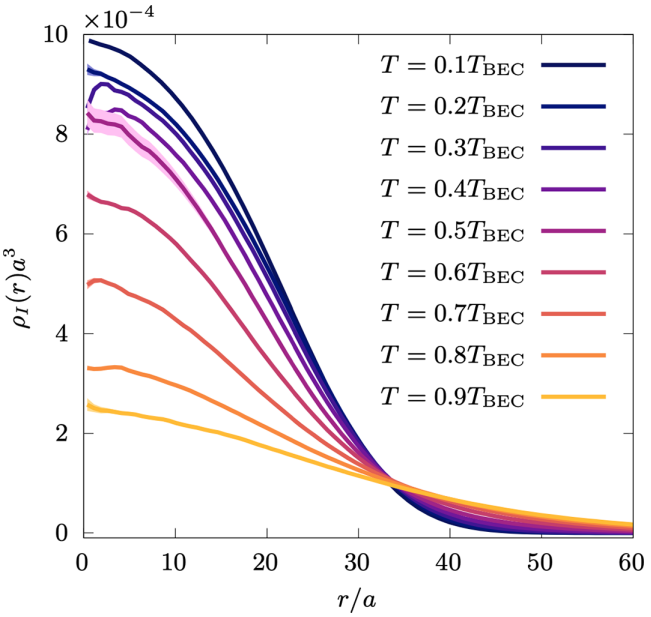

FIG. 6. Density profiles of the particles in the bath at different temperatures with $g_{BI}/g = 1.5$ and $a_{ho}/a = 15$.

between impurity properties T_m can be obtained using QMC techniques and, if it is necessary, one can extrapolate the results to systems with a larger number of particles.

The phenomenon identified in this Letter as well as its relation to thermometry can be experimentally observed since, with the current technologies, the properties of the impurities, e.g., its mean position, can be reliably measured. A possible challenge is to introduce only a single impurity to the system but, as we have shown, even with the presence of a few more impurities, the temperature-induced miscibility still persists, making this approach a promising technique for measurements of the temperature in trapped ultracold gases.

The data presented in this article is available from [49].

Acknowledgments. This work has been supported by the Spanish Ministry of University under Grant FPU No. FPU20/00013, the Spanish Ministry of Economics, Industry and Competitiveness under Grant No. PID2020-113565GB-C21, and AGAUR-Generalitat de Catalunya Grant No. 2021-SGR-01411. This research is part of the project No. 2021/43/P/ST2/02911 co-funded by the National Science Centre and the European Union Framework Programme for Research and Innovation Horizon 2020 under the Marie Skłodowska-Curie grant agreement No. 945339.

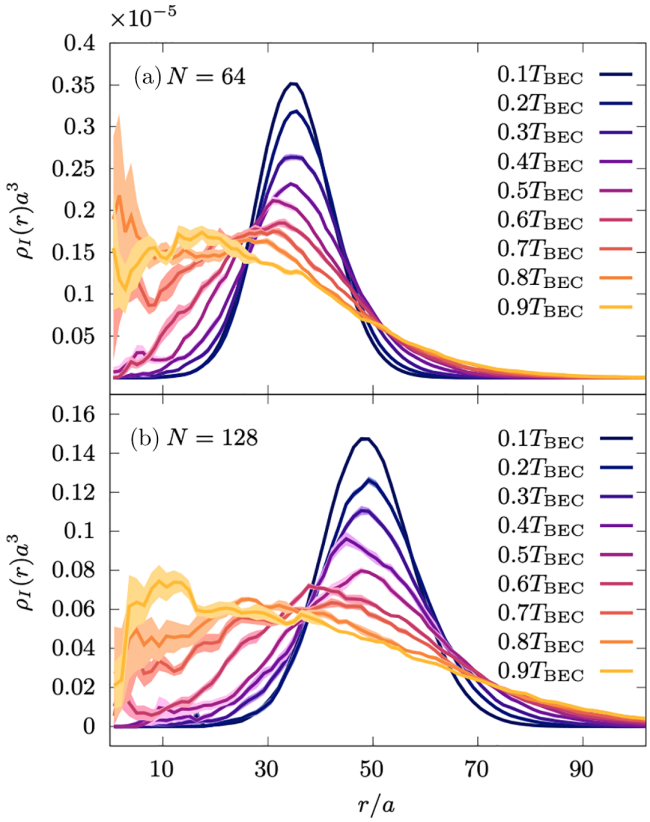

FIG. 7. Density profiles of the impurity at different N with $g_{BI}/g = 3.5$.

Appendix A: Density profiles of the bath. In Fig. 6, we show the density profiles of the particles in the bath at different temperatures. They are normalized to the number of particles ($N = 64$). Notice that the peak of the density profile remains always at the center of the trap.

Appendix B: Finite-size effects. In Fig. 7, we show the differences in the density profiles between a system with $N = 64$ and another with $N = 128$ particles (keeping constant the harmonic confinement). Notice that the impurity moves to further distances when we increase N, as more particles in the bath are expelling it from the center [see Eq. (5) where we show the dependence of the position of the impurity as a function of N]. However, we do not notice a significance change in the mixing temperature T_m.

[1] S. P. Rath and R. Schmidt, Field-theoretical study of the Bose polaron, Phys. Rev. A **88**, 053632 (2013).

[2] W. Li and S. Das Sarma, Variational study of polarons in Bose-Einstein condensates, Phys. Rev. A **90**, 013618 (2014).

[3] F. Grusdt, Y. E. Shchadilova, A. N. Rubtsov, and E. Demler, Renormalization group approach to the Fröhlich polaron model: application to impurity-BEC problem, Sci. Rep. **5**, 12124 (2015).

[4] L. A. Peña Ardila and S. Giorgini, Impurity in a Bose-Einstein condensate: Study of the attractive and repulsive branch using quantum Monte Carlo methods, Phys. Rev. A **92**, 033612 (2015).

[5] A. G. Volosniev, H.-W. Hammer, and N. T. Zinner, Real-time dynamics of an impurity in an ideal Bose gas in a trap, Phys. Rev. A **92**, 023623 (2015).

[6] J. Levinsen, M. M. Parish, and G. M. Bruun, Impurity in a Bose-Einstein condensate and the Efimov effect, Phys. Rev. Lett. **115**, 125302 (2015).

[7] Y. E. Shchadilova, R. Schmidt, F. Grusdt, and E. Demler, Quantum dynamics of ultracold Bose polarons, Phys. Rev. Lett. **117**, 113002 (2016).

[8] N. B. Jørgensen, L. Wacker, K. T. Skalmstang, M. M. Parish, J. Levinsen, R. S. Christensen, G. M. Bruun, and J. J. Arlt, Observation of attractive and repulsive polarons in a Bose-Einstein condensate, Phys. Rev. Lett. **117**, 055302 (2016).

[9] M.-G. Hu, M. J. Van de Graaff, D. Kedar, J. P. Corson, E. A. Cornell, and D. S. Jin, Bose polarons in the strongly interacting regime, Phys. Rev. Lett. **117**, 055301 (2016).

[10] L. A. Peña Ardila and S. Giorgini, Bose polaron problem: Effect of mass imbalance on binding energy, Phys. Rev. A **94**, 063640 (2016).

[11] M. Sun, H. Zhai, and X. Cui, Visualizing the Efimov correlation in Bose polarons, Phys. Rev. Lett. **119**, 013401 (2017).

[12] S. M. Yoshida, S. Endo, J. Levinsen, and M. M. Parish, Universality of an impurity in a Bose-Einstein condensate, Phys. Rev. X **8**, 011024 (2018).

[13] S. Van Loon, W. Casteels, and J. Tempere, Ground-state properties of interacting Bose polarons, Phys. Rev. A **98**, 063631 (2018).

[14] S. I. Mistakidis, G. C. Katsimiga, G. M. Koutentakis, Th. Busch, and P. Schmelcher, Quench dynamics and orthogonality catastrophe of Bose polarons, Phys. Rev. Lett. **122**, 183001 (2019).

[15] T. Ichmoukhamedov and J. Tempere, Feynman path-integral treatment of the Bose polaron beyond the Fröhlich model, Phys. Rev. A **100**, 043605 (2019).

[16] M. Drescher, M. Salmhofer, and T. Enss, Theory of a resonantly interacting impurity in a Bose-Einstein condensate, Phys. Rev. Res. **2**, 032011(R) (2020).

[17] J. Levinsen, L. A. Peña Ardila, S. M. Yoshida, and M. M. Parish, Quantum behavior of a heavy impurity strongly coupled to a Bose gas, Phys. Rev. Lett. **127**, 033401 (2021).

[18] P. Massignan, N. Yegovtsev, and V. Gurarie, Universal aspects of a strongly interacting impurity in a dilute Bose condensate, Phys. Rev. Lett. **126**, 123403 (2021).

[19] F. Isaule, I. Morera, P. Massignan, and B. Juliá-Díaz, Renormalization-group study of Bose polarons, Phys. Rev. A **104**, 023317 (2021).

[20] A. Christianen, J. I. Cirac, and R. Schmidt, Chemistry of a light impurity in a Bose-Einstein condensate, Phys. Rev. Lett. **128**, 183401 (2022).

[21] A. Christianen, J. I. Cirac, and R. Schmidt, Bose polaron and the Efimov effect: A Gaussian-state approach, Phys. Rev. A **105**, 053302 (2022).

[22] M. G. Skou, K. K. Nielsen, T. G. Skov, A. M. Morgen, N. B. Jørgensen, A. Camacho-Guardian, T. Pohl, G. M. Bruun, and J. J. Arlt, Life and death of the Bose polaron, Phys. Rev. Res. **4**, 043093 (2022).

[23] J. Tempere, W. Casteels, M. K. Oberthaler, S. Knoop, E. Timmermans, and J. T. Devreese, Feynman path-integral treatment of the BEC-impurity polaron, Phys. Rev. B **80**, 184504 (2009).

[24] N.-E. Guenther, P. Massignan, M. Lewenstein, and G. M. Bruun, Bose polarons at finite temperature and strong coupling, Phys. Rev. Lett. **120**, 050405 (2018).

[25] V. Pastukhov, Polaron in the dilute critical Bose condensate, J. Phys. A: Math. Theor. **51**, 195003 (2018).

[26] B. Field, J. Levinsen, and M. M. Parish, Fate of the Bose polaron at finite temperature, Phys. Rev. A **101**, 013623 (2020).

[27] Z. Z. Yan, Y. Ni, C. Robens, and M. W. Zwierlein, Bose polarons near quantum criticality, Science **368**, 190 (2020).

[28] G. Pascual and J. Boronat, Quasiparticle nature of the Bose polaron at finite temperature, Phys. Rev. Lett. **127**, 205301 (2021).

[29] M. Mehboudi, A. Lampo, C. Charalambous, L. A. Correa, M. A. García-March, and M. Lewenstein, Using polarons for sub-nK quantum nondemolition thermometry in a Bose-Einstein condensate, Phys. Rev. Lett. **122**, 030403 (2019).

[30] P. Ao and S. T. Chui, Binary Bose-Einstein condensate mixtures in weakly and strongly segregated phases, Phys. Rev. A **58**, 4836 (1998).

[31] M. Ota, S. Giorgini, and S. Stringari, Magnetic phase transition in a mixture of two interacting superfluid Bose gases at finite temperature, Phys. Rev. Lett. **123**, 075301 (2019).

[32] M. Ota and S. Giorgini, Thermodynamics of dilute Bose gases: Beyond mean-field theory for binary mixtures of Bose-Einstein condensates, Phys. Rev. A **102**, 063303 (2020).

[33] G. Spada, L. Parisi, G. Pascual, N. G. Parker, T. P. Billam, S. Pilati, J. Boronat, and S. Giorgini, Phase separation in binary Bose mixtures at finite temperature, SciPost Phys. **15**, 171 (2023).

[34] G. Pascual, G. Spada, S. Pilati, S. Giorgini, and J. Boronat, Thermally induced local imbalance in repulsive binary Bose mixtures, Phys. Rev. Res. **5**, L032041 (2023).

[35] K. Dželalija, V. Cikojević, J. Boronat, and L. Vranješ Markić, Trapped Bose-Bose mixtures at finite temperature: A quantum Monte Carlo approach, Phys. Rev. A **102**, 063304 (2020).

[36] S. Pilati, K. Sakkos, J. Boronat, J. Casulleras, and S. Giorgini, Equation of state of an interacting Bose gas at finite temperature: A path-integral Monte Carlo study, Phys. Rev. A **74**, 043621 (2006).

[37] L. D. Landau and E. M. Lifshitz, *Quantum Mechanics (Nonrelativistic Theory)* (Pergamon Press, Oxford, UK, 1977), p. 550.

[38] S. Giorgini, J. Boronat, and J. Casulleras, Ground state of a homogeneous Bose gas: A diffusion Monte Carlo calculation, Phys. Rev. A **60**, 5129 (1999).

[39] D. M. Ceperley, Path integrals in the theory of condensed helium, Rev. Mod. Phys. **67**, 279 (1995).

[40] S. A. Chin and C. R. Chen, Gradient symplectic algorithms for solving the Schrödinger equation with time-dependent potentials, J. Chem. Phys. **117**, 1409 (2002).

[41] K. Sakkos, J. Casulleras, and J. Boronat, High order Chin actions in path integral Monte Carlo, J. Chem. Phys. **130**, 204109 (2009).

[42] M. Boninsegni, N. V. Prokof'ev, and B. V. Svistunov, Worm algorithm and diagrammatic Monte Carlo: A new approach to continuous-space path integral Monte Carlo simulations, Phys. Rev. E **74**, 036701 (2006).

[43] L. Pitaevskii and S. Stringari, *Bose-Einstein Condensation and Superfluidity* (Oxford University Press, Oxford, UK, 2016).

[44] V Cikojević, L. V. Markić, and J. Boronat, Harmonically trapped Bose-Bose mixtures: a quantum Monte Carlo study, New J. Phys. **20**, 085002 (2018).

[45] E. Krotscheck, M. Saarela, and J. L. Epstein, Impurity states in liquid-helium films, Phys. Rev. B **38**, 111 (1988).

[46] B. E. Clements, E. Krotscheck, and M. Saarela, Impurity dynamics in boson quantum films, Phys. Rev. B **55**, 5959 (1997).

[47] A. F. Andreev, Surface tension of weak helium isotope solutions, J. Exptl. Theoret. Phys. (U.S.S.R.) **50**, 1415 (1966) [Sov. Phys. JETP **23**, 939 (1966)].

[48] J. Lekner, Theory of surface states of ^{3}He atoms in liquid ^{4}He, Philos. Mag. **22**, 669 (1970).

[49] G. Pascual, T. Wasak, A. Negretti, G. E. Astrakharchik, and J. Boronat, Datasets for "Temperature-induced miscibility of impurities in trapped Bose gases" (RepOD, 2024), https://doi.org/10.18150/SRFRWA.